ELSEVIER

Journal of Alloys and Compounds 452 (2008) 389–396

Journal of ALLOYS AND COMPOUNDS

www.elsevier.com/locate/jallcom

Synthesis and characterization of the metal-doped high-voltage spinel $LiNi_{0.5}Mn_{1.5}O_4$ by mechanochemical process

Si Hyoung Oh *, Sang Hoon Jeon, Won Il Cho, Chang Sam Kim, Byung Won Cho

Battery Research Center, Korea Institute of Science and Technology, P.O. Box 131, Cheongryang, Seoul 136-791, Republic of Korea

Received 29 June 2006; received in revised form 18 October 2006; accepted 28 October 2006
Available online 4 December 2006

Abstract

The electrochemical performance of the high-voltage spinel $LiNi_{0.5}Mn_{1.5}O_4$ was improved by doping the original material with the transition metal ion such as trivalent chromium, Cr^{3+}, which had larger bonding strength with oxygen and no Jahn–Teller effect. These high-voltage spinel compounds were prepared by the mechanochemical process, and the synthetic condition was optimized for the best electrochemical performance. It is believed that the high homogeneity of the mixture prepared by mechanical activation helps the synthesis of the phase-pure $LiNi_{0.5-x}Mn_{1.5-y}M_{x+y}O_4$ compound. The doping with the transition metal can enhance the electrochemical properties of $LiNi_{0.5}Mn_{1.5}O_4$ because the large bonding energy between the transition metal and the oxygen prevents the doped spinel from being oxygen-deficient during the high temperature synthesis process, leading to the structural and chemical stability in $LiNi_{0.5}Mn_{1.5}O_4$. The XRD patterns for the doped materials exhibited no impurity phase such as $Li_zNi_{1-z}O$ commonly found in original $LiNi_{0.5}Mn_{1.5}O_4$ probably due to this structural stability of the doped materials. In addition, it is inferred that the improved cyclic performance is mainly attributed to the reduction of the Jahn–Teller distortion by substituting some portion of the high spin Mn^{3+} ions with other transition metal and less Mn dissolution of the doped spinel into the electrolyte, which effectively reduces the increase of impedance during the electrochemical cycling.

Keywords: Energy storage materials; Mechanical alloying; Electrochemical reactions; X-ray diffraction

1. Introduction

Recently, nickel-substituted manganese spinel, $LiNi_{0.5}Mn_{1.5}O_4$ has been intensively studied as one of the most promising alternatives for the cathode materials of the fast-growing high-power lithium secondary batteries [1–11]. This material especially has attracted people's attention because it exhibits the highest practical 5 V capacity compared with other high-voltage class cathode materials such as spinel $LiM_{0.5}Mn_{1.5}O_4$ (M = Cu [12,13], Co [14,15], Fe [13,16]), inverse spinel $LiNiVO_4$ [17], olivine-structured $LiCoPO_4$ [18] and so on. The origin of the high voltage plateau of $LiNi_xMn_{2-x}O_2$ type spinel compound was ascribed to the difference (~0.5 eV) in binding energy of the top valence band between nickel Ni^{2+} 3d e_g (↑↓) and manganese Mn^{3+} 3d e_g (↑) level observed from the ultraviolet photoelectron spectroscopic study [3].

But, it has been reported that spinel $LiNi_{0.5}Mn_{1.5}O_4$ material shows a non-negligible capacity fading during the electrochemical cycling due to the structural and chemical instabilities resulting from the high spin Mn^{3+} ions, which is closely related with the oxygen deficiency of the spinel compound and the formation of impurity phases during the heat treatment process at the high temperatures [2,4,9]. In an ideal case, no Mn^{3+} ions should be present in the stoichiometric compound, $LiNi_{0.5}Mn_{1.5}O_4$, and all Mn^{3+} ions should be substituted by Ni^{2+} ions. However, small amount of Mn^{3+} is often observed in the compound after the high temperature heat-treatment, leading to the advent of nickel-oxide-like peaks in its X-ray diffraction (XRD) patterns and the existence of 4 V capacity in the cyclic voltammogram [2,4,5,9] Past studies by some workers indicated that the extent of Ni substitution for Mn^{3+} in spinel $LiNi_xMn_{2-x}O_4$ structure has a solubility limit around $x \approx 0.5$ and an extra amount of Ni beyond this limit could only exist as impurity phases such as $Li_zNi_{1-z}O$ ($z \approx 0.2$) [4]. Other research group has noted that the manganese valence state in $LiNi_{0.5}Mn_{1.5}O_4$ is highly susceptible to the synthetic temperature range or the cooling rate of heat-treatment process [2]. They

* Corresponding author. Tel.: +82 2 958 5226; fax: +82 2 958 5229.
E-mail address: sho74@kist.re.kr (S.H. Oh).

0925-8388/$ – see front matter © 2006 Elsevier B.V. All rights reserved.
doi:10.1016/j.jallcom.2006.10.153

say that manganese ion is easy to be trivalent above a certain critical temperature level, and through a proper annealing process, small amount of Mn^{3+} ions, which is regarded to be greatly detrimental for the electrochemical and structural property, left in the compound can be completely transformed into Mn^{4+}.

In this study, we have optimized the synthetic conditions of metal-doped $LiNi_{0.5}Mn_{1.5}O_4$ through a mechanochemical process, and the structural and the electrochemical characteristics of the synthesized compound were investigated. It has been known that by introducing an appropriate doping element like chromium, which has large bond dissociation energy (or bond strength) with oxygen, the formation of impurity phases can be efficiently suppressed by relieving oxygen deficiency at the high temperature during the heat-treatment [4,9,13]. Besides, the effect of Jahn–Teller distortion of Mn^{3+} during the electrochemical cycling can be significantly mitigated by the substitution of trivalent Mn^{3+} with the other transition metal ion such as Cr^{3+}, which has only three electrons in its 3d energy level and therefore retains no Jahn–Teller distortion. The mechanochemical process or high-energy ball milling is a common method to prepare a highly homogenous mixture of powders of several species through mechanical activation [10,19–22]. It is believed that the frictional energy triggered by the movement of the balls and powders and the rotation of the bowl, promotes certain chemical reactions between the raw particles. The conventional solid-state method to synthesize the high-performance $LiNi_{0.5}Mn_{1.5}O_4$ has been reported unsuccessful so far due to the formation of nickel-oxide-like phases and the chemical instabilities of Mn^{3+} ions with electrolyte, resulting from the local inhomogeneity in the microchemistry and the large diffusion path between the particles during synthetic process [2,4,5].

2. Experimental procedure

The mechanochemical process was employed to synthesize the high-performance $LiNi_{0.5-x}Mn_{1.5-y}M_{x+y}O_4$ (M = Cr, Ti, Fe, Zn) cathode material, in which planetary-type ball mill was adopted for the mechanical activation of the starting materials. Proper amount of Li_2CO_3, MnO_2, $Ni(OH)_2$ together with small amount of the doping materials such as Cr_2O_3, TiO_2, Fe_2O_3, and ZnO was weighed and poured into 500 ml zirconia bowl at the same time. Considering ball to powder ratio (BPR) equal to 5:1, zirconia ball with Ø 10 mm, was weighed and also put into the same bowl. After that, the powder was ball-milled at a speed of 400 rpm for 30 min. Thermogravimetric analysis (TGA) and differential scanning calorimetry (DSC) were performed in the air atmosphere at a heating rate of 5 °C/min for the starting materials to determine a relevant heat schedule. After that, the ball-milled powder was collected and subjected to further two-step heat treatment at 600 °C for 8 h in air and subsequently, at 800–900 °C for 12 h in the air or sometimes in the flowing oxygen atmosphere.

Structural properties of the synthesized compounds were studied by the X-ray diffraction technique (XRD). The surface and particle morphology of the synthesized materials were analyzed by scanning electron microscopy (SEM) images. The electrochemical cycling performance of the materials was studied by assembling coin-type cells (CR2032) and the cells were galvanostatically cycled at a 0.5 C rate (1C = 147 mA/g) between 3.5 and 5.0 V in a multi-channel battery tester. The cyclic voltammogram was obtained by scanning the cell at a slow rate of 20 μV/s. The synthesized cathode materials were mixed with 10% carbon black and 3% polyvinylidene fluoride (PVdF) as a binder, and made into a slurry using *N*-methylpyrrolidinone (NMP) as a solvent and coated onto aluminum foil which was used as a current collector. The typical loading rate of active materials was about 7.5 mg/cm^2 with 40–50 μm thickness. The coated aluminum foil was allowed to dry in hot oven at 80 °C and then it was roller pressed to better adhere the materials to the current collector. The cathodes were punched from the foil. The cells were assembled inside drying room using lithium metal as an anode, polypropylene (PP) film as a separator and a 1 M $LiPF_6$ in 1:1:1 ethylene carbonate (EC), ethylmethyl carbonate (EMC), dimethyl carbonate (DMC) co-solvent as an electrolyte.

3. Results and discussion

The thermogravimetric behavior of the starting materials for the synthesis of $LiNi_{0.5}Mn_{1.5}O_4$ was shown in Fig. 1(a and b). The source materials for the major transition metal components Ni, Mn, dissociated rapidly at the relatively low temperature region, while lithium carbonate remained intact up to 700 °C. The oxide doping materials such as Cr_2O_3 showed little weight gain or loss throughout the temperature scan, for which TG data were therefore left out here. However, it seems that the TG and DSC data for the mixed power indicates that the major synthetic process occurs below 600 °C and about 18% of the initial starting materials, is burned up during the firing, which is in good agreement with the mathematical calculation considering the weight loss between the initial and the final materials involved ($Li_2CO_3 + MnO_2 + Ni(OH)_2 \rightarrow LiNi_{0.5}Mn_{1.5}O_4$). From Fig. 1a, it seems that quadrivalent manganese oxide MnO_2 dissociates abruptly around 550 °C to become trivalent Mn_2O_3

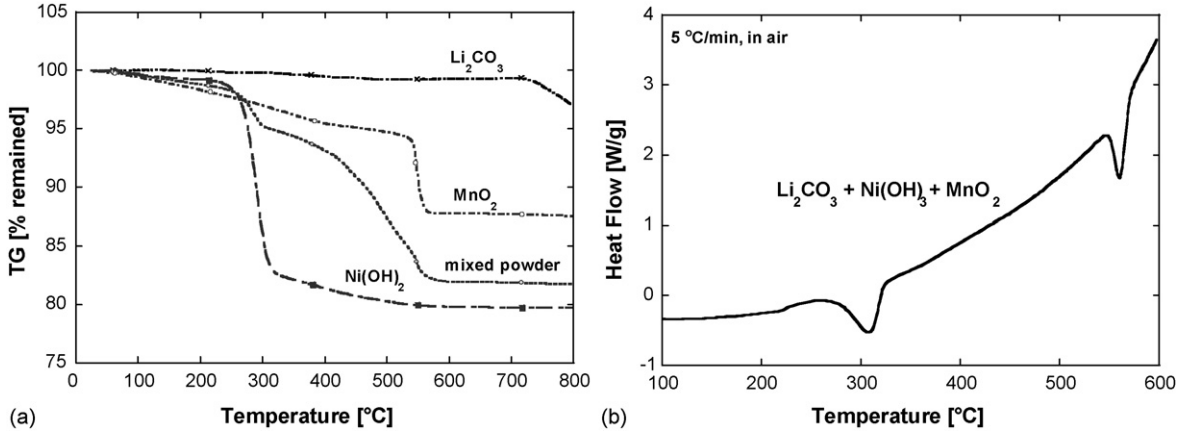

Fig. 1. (a) TGA results for the starting materials, Li_2CO_3, $Ni(OH)_2$, MnO_2, and the mixed powder and (b) DSC results for the mixed powder.

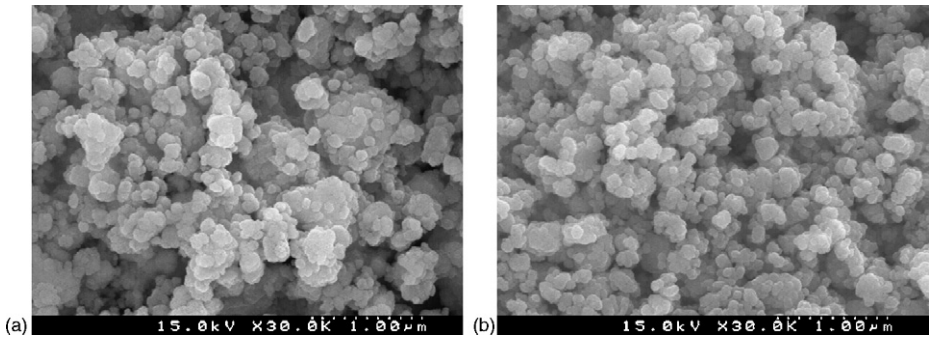

Fig. 2. SEM images of the intermediate compound for synthesizing $LiNi_{0.5}Mn_{1.5}O_4$: (a) as ball-milled powder and (b) power after heat-treatment at 600 °C for 8 h.

($2MnO_2 \rightarrow Mn_2O_3 + 1/2O_2$), which implies that Mn^{3+} ion is more stable than Mn^{4+} in the high temperature region above this temperature. This unique feature of the manganese oxide suggests that the insufficient homogeneity of the mixed powder can result in the formation of Mn^{3+} in the $LiNi_{0.5}Mn_{1.5}O_4$ compound during the high temperature calcination, which is regarded to be detrimental in the structural and chemical stability with electrolyte and results in the capacity fading in the electrochemical test.

In Fig. 2a, the microstructure of the ball-milled powder reveals the agglomerate structure of primary particles with submicron size around 0.1–0.2 μm, which may result from the fact that the high-energy of ball milling induces the fracture and homogeneous mixing of the starting materials. Besides, although the powder after heat-treatment at 600 °C shows little difference from the just ball-milled powder, XRD patterns in Fig. 3 indicate that the significant crystallographic development occurs after the heat-treatment at 600 °C. That is, the XRD pattern for just ball-milled powder (Fig. 3a) shows broad and ambiguous peaks, whereas that for the powder after heat-treatment (Fig. 3b) shows the typical peaks observed in the spinel structure. The sharp and more developed peaks in Fig. 3c denote further crystallization of the spinel structure in higher temperatures.

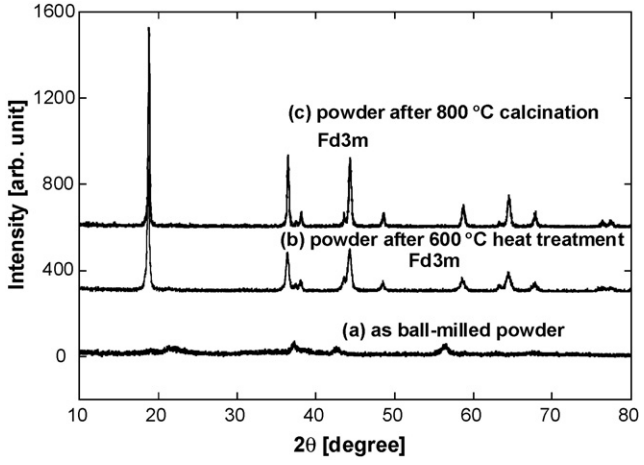

Fig. 3. X-ray diffraction patterns for the intermediate and final compounds during the synthetic process of $LiNi_{0.5}Mn_{1.5}O_4$ materials: (a) as ball-milled powder, (b) powder after heat treatment at 600 °C and (c) and powder after heat treatment at 800 °C.

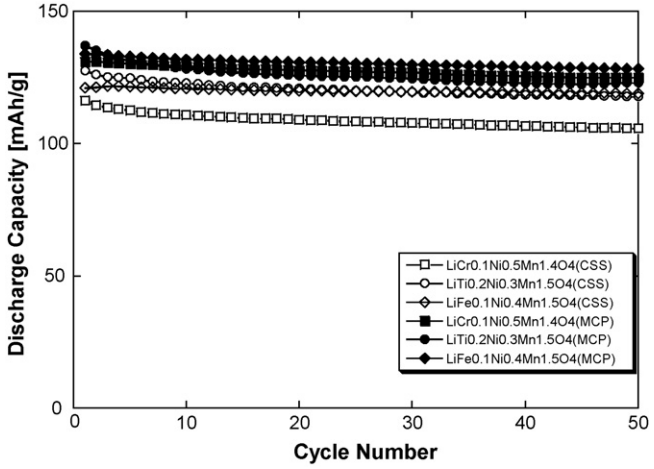

Fig. 4. (a) Cyclic performance of the cells made of $LiNi_{0.5-x}Mn_{1.5}M_xO_4$ (M = Mn, Cr, Fe, Ti, Zn) cathode materials synthesized by conventional solid-state method (CSS) and by mechanochemical process (MCP).

The effect of the mechanochemical activation on the electrochemical performance of the synthesized powder of various compositions is shown in Fig. 4. It was found that the specific discharge capacities of the all cathode materials synthesized by MCP were substantially greater than those by conventional solid-state method although both of the two synthetic processes showed relatively good cyclic capacity retention of more than 90% at the 50th cycle. This may reflect the fact that the high energy of the ball milling promoted the mixing and the homogenization between the starting materials, which helped the synthesis of good crystalline cathode materials.

The composition of the synthesized powder $LiNi_{0.5}Mn_{1.5}O_4$, $LiCr_{0.1}Ni_{0.4}Mn_{1.5}O_4$ was analyzed through the ICP and AAS, and the results were tabulated in Table 1. Both powders from the conventional solid-state method and MCP showed a reasonably good agreement with the targeted composition although

Table 1
The result of elemental analysis of the compounds by ICP&AAS

Material/element	Li	Ni	Mn	Cr	Zr
$LiNi_{0.5}Mn_{1.5}O_4$[a]	0.98	0.50	1.50	–	–
$LiNi_{0.5}Mn_{1.5}O_4$	0.99	0.50	1.50	–	–
$LiCr_{0.1}Ni_{0.4}Mn_{1.5}O_4$	1.03	0.40	1.51	0.09	4.52E−04

[a] Synthesized by conventional solid state method.

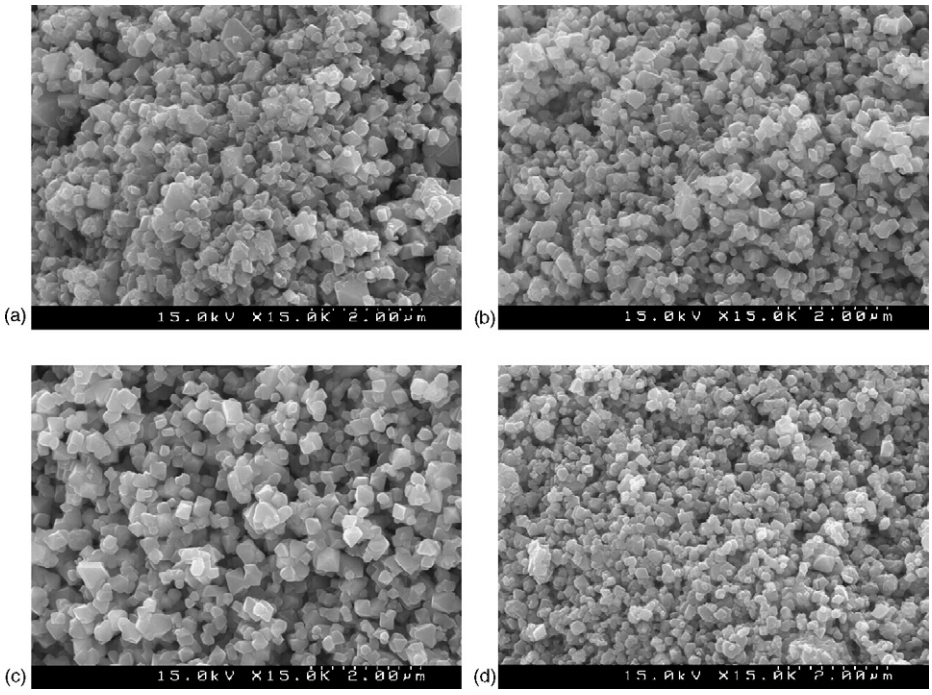

Fig. 5. SEM images for: (a) $LiCr_{0.1}Ni_{0.4}Mn_{1.5}O_4$, (b) $LiFe_{0.1}Ni_{0.4}Mn_{1.5}O_4$, (c) $LiTi_{0.2}Ni_{0.3}Mn_{1.5}O_4$ and (d) $LiZn_{0.1}Ni_{0.4}Mn_{1.5}O_4$.

the lithium contents were a little smaller than the expected in case of $LiNi_{0.5}Mn_{1.5}O_4$. The amount of zirconium contents in $LiCr_{0.1}Ni_{0.4}Mn_{1.5}O_4$ were checked to confirm if any impurity should be introduced from the balls and bowl during the ball-mill process. According to the analysis, very small amount of zirconium was detected (less than 5×10^{-4}), which can be regarded to have a negligible effect on the electrochemical performance and it can be said that the contamination from the bowl and ball counts little.

Fig. 5(a–d) describes the morphological variations of the $LiNi_{0.5-x}Mn_{1.5}M_xO_4$ (M = Cr, Fe, Ti, Zn) compound synthesized at 800 °C for 12 h by the mechanochemical process. As shown in the figure, all the compounds exhibit similar octahedral shapes generally found in the spinel structure with a primary particle size around 0.1–0.2 μm regardless of their compositions. Thus, these materials are believed to harbor a good crystallinity.

The X-ray diffraction patterns for analyzing the crystallographic structure and the impurity phases of the doped compounds synthesized by mechanochemical process are shown in Fig. 6(a and b). For this analysis, six types of spinel compounds have been prepared, each sample possessing a different composition or a preparing condition, which is tabulated in Table 2. The bare (Nos. 2 and 3) and the chromium-doped $LiNi_{0.5}Mn_{1.5}O_4$ (Nos. 4–6) compounds with a different calcination atmosphere were prepared to investigate the effect of transition metal doping and the contribution of the oxygen partial pressure during the calcination process on the spinel structure. The $LiMn_2O_4$ compound (No. 1), where Mn^{3+} ion has the same population with Mn^{4+}, and thus has strong Jahn–Teller dis-

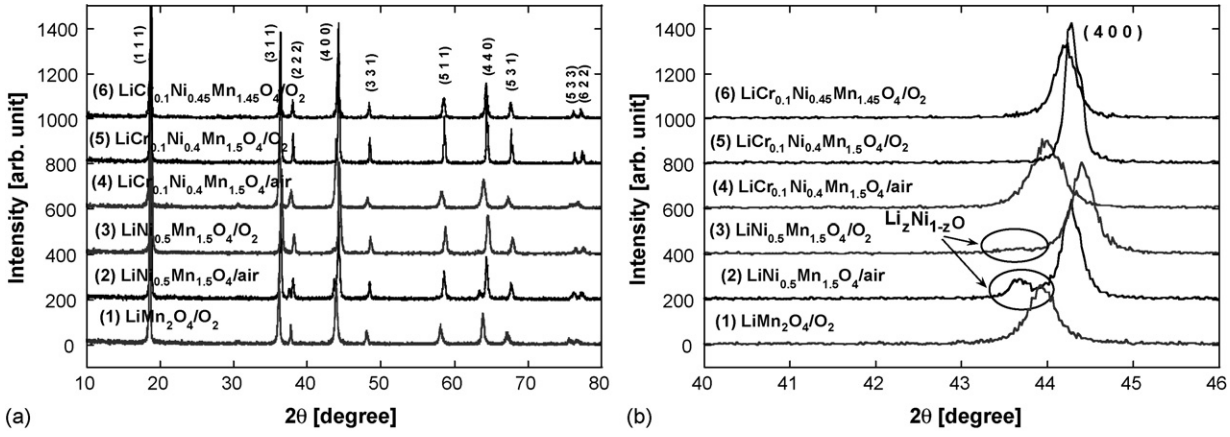

Fig. 6. X-ray diffraction patterns for series of $LiNi_{0.5-x}Mn_{1.5}Mn_xO_4$ (M = Mn, Cr) materials synthesized by mechanochemical process: (a) XRD patterns (10–80 °C) and (b) near (4 0 0) peak.

Table 2
The nominal compositions of the compounds synthesized for the analysis of X-ray diffraction pattern and their expected valence states of transition metals (TM)

Sample no.	Composition	Aimed valence state of TM	Heat treatment/atmosphere
1	$LiMn_2O_4$	$[Mn^{3+}]_{1.0}[Mn^{4+}]_{1.0}$	Calcined at 800 °C in O_2
2	$LiNi_{0.5}Mn_{1.5}O_4$	$[Ni^{2+}]_{0.5-x}[Mn^{3+}]_{2x}[Mn^{4+}]_{1.5-x}$	Calcined at 800 °C in air
3	$LiNi_{0.5}Mn_{1.5}O_4$	$[Ni^{2+}]_{0.5}[Mn^{4+}]_{1.5}$	Calcined at 800 °C in O_2
4	$LiCr_{0.1}Ni_{0.40}Mn_{1.50}O_4$	$[Cr^{3+}]_{0.1}[Ni^{2+}]_{0.4}[Mn^{3+}]_{0.1}[Mn^{4+}]_{1.4}$	Calcined at 800 °C in air
5	$LiCr_{0.1}Ni_{0.40}Mn_{1.50}O_4$	$[Cr^{3+}]_{0.1}[Ni^{2+}]_{0.4}[Mn^{3+}]_{0.1}[Mn^{4+}]_{1.4}$	Calcined at 800 °C in O_2
6	$LiCr_{0.1}Ni_{0.45}Mn_{1.45}O_4$	$[Cr^{3+}]_{0.1}[Ni^{2+}]_{0.45}[Mn^{4+}]_{1.45}$	Calcined at 800 °C in O_2

tortions and larger lattice parameters, was synthesized for the comparison with the high voltage spinels. Table 2 also shows the targeted valence state of transition metal in the synthesized compound, where the valence states of the nickel and the chromium are assumed to be fixed to +2 and +3, respectively, whereas that of manganese can become +3 or +4 depending on the compound composition and synthetic conditions. Because it has been known that the substitution of Cr in $LiMn_{2-y}Cr_yO_4$ spinel leads to a conversion of some Cr^{3+} to Cr^{6+}, which is known as undoubtedly noxious species, for $y > 0.2$, and further replacement could result in the formation of $LiCrO_2$ impurity phase ($y > 0.8$) [26], furthermore it has been reported that the electrochemical performance of $LiCr_yNi_{0.5-y}Mn_{1.5}O_4$ cathode improves as chromium contents increases [9], we set the amount of doped chromium to 0.1 for safety in this study.

In Fig. 6a, all the XRD patterns for the compounds prepared by the mechanochemical process showed a good crystallinity with typical peaks commonly observed in *Fd3m* space group except the $LiNi_{0.5}Mn_{1.5}O_4$ compound synthesized in the air, which showed series of distinct impurity peaks in Fig. 6(a and b) related with $Li_zNi_{1-z}O$, compared with other compounds. The $LiNi_{0.5}Mn_{1.5}O_4$ compound synthesized under the O_2 atmosphere also showed a weak hump related with impurity phase in its XRD pattern, but much smaller intensity indicates that the control of oxygen partial pressure has profound effect to eliminate impurity phase and thus suppress Mn^{3+} ions in the compound. The peaks for impurity phase were not observed for the all the doped compounds, where the strong bonding strength of chromium with oxygen is believed to effectively suppress the advent of impurities, which may be related with existence of Mn^{3+} ions in the compound. The Mn^{3+} ions in the spinel structure induce repeated Jahn–Teller distortion as well as redundant 4 V capacity due to the Mn^{3+}/Mn^{4+} redox reaction near 4.1 V during the electrochemical test.

The lattice parameters a_0 for all the compounds, calculated by the least square method using the 10 major diffraction lines from the XRD pattern, were shown in Table 3. As depicted in the table, all the high-voltage spinel materials have significantly smaller lattice parameters than $LiMn_2O_4$ (No. 1) due to the elimination of big Mn^{3+} ions, in the spinel structure. Because it is believed that $LiNi_{0.5}Mn_{1.5}O_4$ compound (No. 2) calcined in the air carries more Mn^{3+} ions than No. 3 synthesized in O_2 atmosphere does, the lattice parameter of this No. 2 compound was slightly larger since the ionic size of Mn^{4+}(0.530 Å) is much smaller than Mn^{3+}(0.645 Å) [4,23]. Besides, because the ionic radius of Cr^{3+} are 0.615 Å, which is a little smaller than that of Mn^{3+}, the doped material (No. 4–6) showed relatively small lattice parameters compared with the bare materials containing large amount of Mn^{3+} ions (No. 2), but they exhibited larger lattice parameter than No. 3 compound, which has small Mn^{3+} ions in its structure. This may be explained by the fact that the lattice parameters of the high voltage spinels are likely to depend on the amount of Mn^{3+} ions within the spinel structure, while doping materials contributes just a small portion to the overall spinel structure [2,4].

Table 3
The lattice parameters of various compositions of $LiNi_{0.5-x}Mn_{1.5}M_xO_4$ compounds synthesized by the mechanochemical process shown in Table 2

Sample no.	1	2	3	4	5	6
a_0 (Å)	8.2422	8.1959	8.1657	8.1888	8.1663	8.1757

It has been pointed out that by doping a relevant transition metal like chromium, which has large bond dissociation energy with the oxygen, the formation of impurity phases can be controlled by reducing the oxygen deficiency at the high temperature during the calcination [4,9,13], and the substitution of some portion of nickel by other transition metal works out the solubility problem of nickel into the spinel structure [4], which was verified by the XRD patterns in Fig. 6a. In addition, the harmful effect of Jahn–Teller distortion of Mn^{3+} ion during the electrochemical cycling can be well enough mitigated by the substitution of Mn^{3+} with other transition metal ion such as Cr^{3+}, which has only three electrons in its 3d t_{2g} (↑) energy level and therefore retains no Jahn–Teller distortion. It is inferred that this structural stability of the doped spinel also enhances the chemical stability of Mn^{3+} with electrolyte at the interface, and less Mn dissolution occurs ($Mn^{3+} \rightarrow Mn^{4+} + Mn^{2+}$(sol)). Table 4 shows the bond dissociation energies and the ionic radii for the various transition metals involved with the high-voltage spinel such as Mn, Ni, Cr, Fe, Ti, and Zn. Because the doping metal replaces Mn^{3+} or Ni^{2+} in the spinel structure, similar ionic radius (for example, Cr^{3+}, Ti^{4+}) for the doping metal with Mn^{3+} (or Ni^{2+}) will be favorable to the synthesis of doped materials. From the table, bond strengths of Cr and Ti exceed that of Mn, whereas Fe, Zn has smaller bond strength, which implies that Cr or Ti doped compound will exhibit better electrochemical performance than Fe or Zn doped compounds.

Fig. 7(a and b) shows the cyclic performance and the discharge profiles of the first cycle, for the cells made of $LiNi_{0.5-x}Mn_{1.5}M_xO_4$ (M = Ni, Cr, Fe, Ti, Zn) cathode materials synthesized by the mechanochemical process and a lithium

Table 4
Bond dissociation energies of the representative transition metals with oxygen and the ionic radii of the various transition metals when the coordination number is six

Bond dissociation energies ΔHf(298 K) (kJ/mol)		Ionic radii (CN = 6) of transition metal	
Bond	ΔHf	Valence number	Radius (Å)
Mn—O	402	3+	0.645
		4+	0.530
Ni—O	382	2+	0.690
Cr—O	461	3+	0.615
Fe—O	390	3+	0.550
Ti—O	672	4+	0.610
Zn—O	159	2+	0.740

anode. The cells were cycled between 3.5–5.0 V at C/2 rate (1C = 147 mA/g). As can be seen in Fig. 7a, $LiCr_{0.1}Ni_{0.4}Mn_{1.5}O_4$ compound synthesized in the O_2 atmosphere exhibited the highest gravimetric capacity near 140 mAh/g and the best cyclic stability, while all the other compounds shows some effect in improving the capacity retention. It is believed that the higher bond strength of the chromium with oxygen (467 kJ/mol) than that of Mn–O (402 kJ/mol) played an important role in preventing the compound from being oxygen deficient at the high temperature and reduce the dissolution of manganese ion into electrolyte during the electrochemical cycling, resulting in an improved capacity retentions. It is reported that the dissolution of the transition metal from the cathode material dramatically increases the interfacial impedance of the electrochemical cell during the charge-discharge cycling, and is classified as one of the major deteriorating mechanisms [24,25]. The increased oxygen partial pressure during the calcination is also believed to help overcome the oxygen deficiency problem of the high-voltage spinel. Zn doped spinel, which has low bond strength with oxygen, also showed better cyclic performance than bare material but it suffered from the low initial discharge capacity.

In the discharge profiles in Fig. 7b, all the compounds exhibit substantial fraction of 4 V capacity, originating from the redox reaction of Mn^{3+} existing in the $LiNi_{0.5-x}Mn_{1.5}M_xO_4$ compound or that of the doping element, $M^{\alpha}/M^{\alpha+1}$. The fraction of the contributions from 4 or 5 V capacity to the total discharge capacity was tabulated in Table 5. The bare $LiNi_{0.5}Mn_{1.5}O_4$ compound also exhibited 9% of 4 V capacity. This means that Mn^{3+} ions exist with the $Li_zNi_{1-z}O$ impurity phase (Fig. 6) within the spinel structure and the valence state of the transition metals of this compound can be written as $[Ni^{2+}]_{0.455}[Mn^{3+}]_{0.09}[Mn^{4+}]_{1.455}$ from Table 2. The Cr-doped spinel calcined in oxygen atmosphere just show as much 4 V contributions from Mn^{3+} ions as expected from the composition because the valence state of the transition metal for this material is assumed to be $[Cr^{3+}]_{0.1}[Ni^{2+}]_{0.4}[Mn^{3+}]_{0.1}[Mn^{4+}]_{1.5}$. Other transition metal doped compounds showed an excessive amount of 4 V capacity probably due to the co-existence of

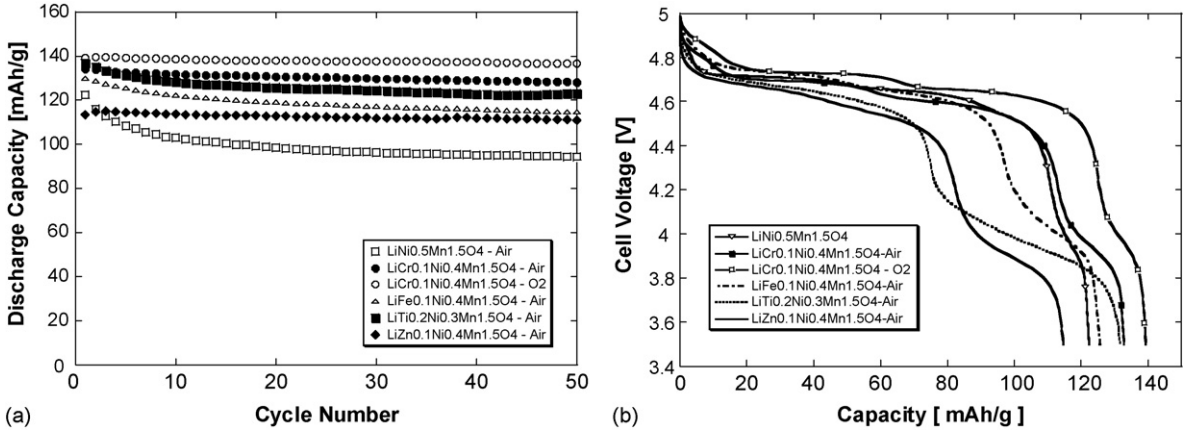

Fig. 7. (a) Cyclic performance and (b) discharge profiles of the cells made of $LiNi_{0.5-x}Mn_{1.5}M_xO_4$ (M = Mn, Cr, Fe, Ti, Zn) cathode materials synthesized by mechanochemical process.

Table 5
4 V and 5 V capacities of the synthesized cathode materials

Sample	Total discharge capacity	<4.2 V		4.75 V > x > 4.2 V		>4.75 V	
		Capacity	Percentage (%)	Capacity	Percentage (%)	Capacity	Percentage (%)
$LiNi_{0.5}Mn_{1.5}O_4$	122.2	11.2	9	106.0	87	5.0	4
$LiCr_{0.1}Ni_{0.4}Mn_{1.5}O_4$	132.7	19.7	15	102.0	77	11.0	8
$LiCr_{0.1}Ni_{0.4}Mn_{1.5}O_4(O_2)$	139.0	13.5	10	105.0	76	20.5	15
$LiFe_{0.1}Ni_{0.4}Mn_{1.5}O_4$	125.5	25.5	20	83.0	66	17.0	14
$LiTi_{0.2}Ni_{0.3}Mn_{1.5}O_4$	131.3	54.3	41	71.0	54	6.0	5
$LiZn_{0.1}Ni_{0.4}Mn_{1.5}O_4$	114.5	32.5	28	79.0	69	3.0	3

Capacity unit, mAh/g.

redox reaction of the doping element $M^{\alpha}/M^{\alpha+1}$ together with Mn^{3+}/Mn^{4+} redox couple. In fact, it has been reported that among the 5 V class spinel compounds typed $LiM_{0.5}Mn_{1.5}O_4$, only $LiNi_{0.5}Mn_{1.5}O_4$ compound holds all of its capacity in the 5 V region [1,11]. Therefore, it is reasonable to assume that the extra 4 V capacity of the Fe, Ti or Zn doped spinels in Fig. 7b comes from the redox reaction of the doping materials, $M^{\alpha}/M^{\alpha+1}$, which may exist in the low valence state in the spinel structure. Redox reaction from the high valence state of the doping material may be related with 5 V capacity just as $LiFe_{0.5}Mn_{1.5}O_4$ compound exhibits voltage plateaus both in 4 V region (Fe^{2+}/Fe^{3+}) and in 5 V region (Fe^{3+}/Fe^{4+}) with each voltage region possessing a similar capacity [1,13,16]. However, the valence state of the doping material within the spinel structure such as Fe, Zn, and Ti except Cr was not clearly defined or examined in this work, which remained as a future work, while the valence state of Cr in $LiCr_{x+y}Ni_{0.5-x}Mn_{1.5-y}O_4$ compound is assumed to be +3 in mild Cr substitution ($x+y<0.2$) [4].

The cyclic voltammograms were obtained for the compound $LiCr_{x+y}Ni_{0.5-x}Mn_{1.5-y}O_4$ at a scan rate of 0.02 mV/s by switching the ramping voltage at 3.5 and 5.0 V, and are shown in Fig. 8(a–d) to analyze the Cr-doped spinel compound more in detail. From Fig. 8a, it is obvious that the $LiNi_{0.5}Mn_{1.5}O_4$ compound synthesized in the air exhibits Mn^{3+}/Mn^{4+} redox reaction near 4.1 V and has corresponding 4 V capacity. Because $Li_zNi_{1-z}O$-like phase is clearly observed in the XRD pattern in Fig. 6(a and b) (No. 3), the existence of Mn^{3+} ion and the formation $Li_zNi_{1-z}O$ impurity phase seems to be closely interconnected in the $LiNi_{0.5}Mn_{1.5}O_4$ compound. Other researches on this material have indicated that the control of the cooling rate after the high temperature calcination is essential step to remove any Mn^{3+} ion from the spinel structure because the following disproportion reaction will not occur in case of the fast cooling [2,4].

$$LiNi_{0.5}Mn_{1.5}O_4\,(\text{at low } T) \leftrightarrows qLi_zNi_{1-z}O + r\,LiNi_{0.5-w}Mn_{1.5+w}O_4 + sO_2\,(\text{at high } T)$$

They insisted that when the cooling rate after the calcination at the high temperature is very slow or the compound is exposed to an annealing process below a certain critical temperature, Mn^{3+} ions in the compound can be reversibly transformed into Mn^{4+} ion without any nickel oxide-like impurity phase around 600–650 °C.

In case of $LiCr_{0.1}Ni_{0.4}Mn_{1.5}O_4$ compounds (Fig. 8b), there observed significant 4 V peaks related with Mn^{3+}/Mn^{4+} redox reaction in its cyclic voltammogram as expected from the valence state of the transition metal in Table 2. However, the compound synthesized under O_2 atmosphere showed far less amount of 4 V capacity, which implies that higher oxygen

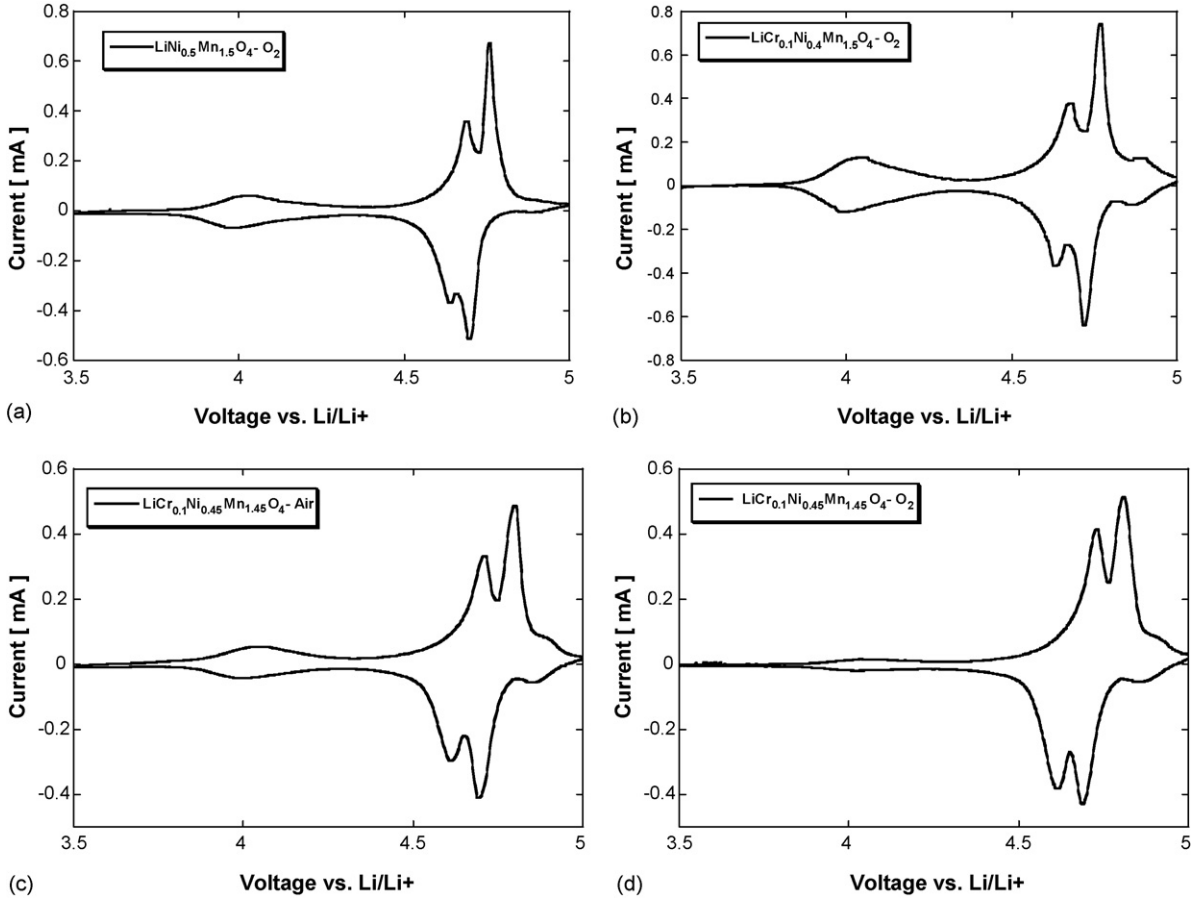

Fig. 8. Cyclic voltammograms for the cells made of the $LiNi_{0.5-x}Mn_{1.5-y}M_{x+y}O_4$ (M = Mn, Cr) cathode materials synthesized by mechanochemical process: (a) $LiNi_{0.5}Mn_{1.5}O_4$, (b) $LiCr_{0.1}Ni_{0.4}Mn_{1.5}O_4$, (c) $LiCr_{0.1}Ni_{0.4}Mn_{1.5}O_4$ (O_2) and (d) $LiCr_{0.1}Ni_{0.45}Mn_{1.45}O_4$.

partial pressure plays a certain role in relieving the oxygen deficiency and suppressing the advent of impurity phase in the spinel structure during the calcination. Besides, this material shows additional redox peaks around 4.9 V resulting from the Cr^{3+}/Cr^{4+} redox couple [1,4,13]. The compound $LiCr_{0.1}Ni_{0.45}Mn_{1.45}O_4$ is considered to a composition free of Mn^{3+} ions as assumed in Table 2 and indeed it exhibited negligible 4 V peaks in Fig. 8d compared with other compounds. This indicates that the Cr doping of the bare material can suppress the generation of Mn^{3+} ions in the high temperature, possibly due to the higher bonding strength between chromium and oxygen than that between the existing Mn–O bond, which may relieve the oxygen deficiency in the spinel compound.

In summary, the high-performance 5 V class spinel-type cathode material was successfully synthesized by employing the mechanochemical process for the homogeneity of the heat-treatment precursor, optimizing the calcination condition, and selecting an appropriate material composition with a proper doping material, which has large bonding strength with oxygen compared with manganese.

4. Conclusion

The electrochemical performance of the high-voltage spinel $LiNi_{0.5}Mn_{1.5}O_4$ was improved by doping the original material with the transition metal ion such as Cr^{3+}, which had larger bonding strength with oxygen and no Jahn–Teller effect. This high-voltage spinel compounds were prepared by means of the mechanochemical process, and the synthetic condition was optimized for the best electrochemical performance. The high homogeneousness of the mixture prepared by mechanical activation helps the synthesis of the phase-pure $LiNi_{0.5-x}Mn_{1.5-y}M_{x+y}O_4$ compound. The doping with the transition metal can enhance the electrochemical properties of $LiNi_{0.5}Mn_{1.5}O_4$ because larger bonding energy between the transition metal and the oxygen prevents the doped spinel from being oxygen-deficient during the high temperature synthesis process, leading to the structural and chemical stability in $LiNi_{0.5}Mn_{1.5}O_4$. The XRD patterns for the doped materials exhibited no impurity phase such as $Li_zNi_{1-z}O$ commonly found in original $LiNi_{0.5}Mn_{1.5}O_4$ probably due to this structural stability of the doped materials. In addition, it is inferred that the improved cyclic performance is mainly attributed to the structural stability due to the reduction of the Jahn–Teller distortion by replacement of some portion of the high spin Mn^{3+} ions by other transition metal and less Mn dissolution of the doped spinel into the electrolyte, which effectively reduces the increase of impedance during the electrochemical cycling.

Acknowledgement

This work was supported by the Core Technology Development Program of the Ministry of Commerce, Industry and Energy (MOCIE).

References

[1] T. Ohzuku, S. Takeda, M. Iwanaga, J. Power Sources 81–82 (1999) 90.
[2] Q. Zhong, A. Bonakdarpour, M. Zhang, Y. Gao, J.R. Dahn, J. Electrochem. Soc. 144 (1997) 205.
[3] Y. Gao, K. Myrtle, M. Zhang, J.N. Reimers, J.R. Dahn, Phys. Rev. B 54 (1996) 16670.
[4] T.A. Arunkumar, A. Manthiram, Electrochim. Acta 50 (2005) 5568.
[5] Y.S. Lee, Y.K. Sun, S. Ota, T. Miyashita, M. Yoshio, Electrochem. Commun. 4 (2002) 989.
[6] F.G.B. Ooms, E.M. Kelder, J. Schoonman, M. Wagemaker, F.M. Mulder, Solid State Ionics 152–153 (2002) 143.
[7] K. Amine, H. Tukamoto, H. Yasuda, Y. Fujita, J. Power Sources 68 (1997) 604.
[8] B. Markovsky, Y. Talyossef, G. Salitra, D. Aurbach, H.J. Kim, S. Choi, Electrochem. Commun. 6 (2004) 821.
[9] S.B. Park, W.S. Eom, W.I. Cho, H. Jang, J. Power Sources 159 (2006) 679.
[10] S.H. Jeon, S.H. Oh, B.J. Lee, W.I. Cho, B.W. Cho, J. Korean Electrochem. Soc. 4 (2005) 170.
[11] H. Kawai, M. Nagata, H. Tukamoto, A.R. West, J. Power Sources 81–82 (1999) 67.
[12] Y. Ein-Eli, S.H. Lu, M.A. Rzeznik, J. Electrochem. Soc. 145 (1998) 3383.
[13] G.T.K. Fey, C.Z. Lu, T.P. Kumar, J. Power Sources 115 (2003) 332.
[14] C. Sigala, D. Guyomard, A. Verbaere, Y. Piffard, M. Tournoux, Solid State Ionics 81 (1995) 167.
[15] H. Kawai, M. Nagata, H. Kageyama, H. Tukamoto, A.R. West, Electrochim. Acta 45 (1999) 315.
[16] H. Kawai, M. Nagata, M. Tabuchi, H. Tukamoto, A.R. West, Chem. Mater. 10 (1998) 837.
[17] G.T.K. Fey, J.R. Dahn, M.J. Zhang, W. Li, J. Power Sources 68 (1997) 549.
[18] S. Okada, S. Sawa, M. Egashira, J. Yamaki, M. Tabuchi, H. Kaheyama, T. Konishi, A. Yoshino, J. Power Sources 97–98 (2001) 430.
[19] W.T. Jeong, K.S. Lee, J. Alloys Compd. 332 (2001) 205.
[20] W.T. Jeong, J.H. Joo, K.S. Lee, J. Alloys Compd. 119–121 (2003) 690.
[21] W.T. Jeong, S.H. Oh, W.I. Cho, B.W. Cho, 206th Meeting of the Electrochemical Society, Abs. No. 404, 2004.
[22] W.T. Jeong, S.H. Oh, H.J. Kim, W.I. Cho, B.W. Cho, 204th Meeting of the Electrochemical Society, Abs. No. 1000, 2003.
[23] R. Lide David, Hanbook of Chemistry and Physics, 83rd ed., 2002, pp. 12–14.
[24] S.H. Oh, S.M. Lee, W.I. Cho, B.W. Cho, Electrochim. Acta 51 (2006) 3637.
[25] D.P. Abraham, R.D. Twesten, M. Balasubramanian, I. Petrov, J. Mcbreen, K. Amine, Electrochem. Commun. 4 (2002) 620.
[26] C. Wu, F. Wu, L. Chen, X. Huang, Solid State Ionics 152–153 (2002) 335.